Saffman-Taylor instability of viscoelastic fluids: From viscous fingering to elastic fractures

S. Mora[*]

*Laboratoire des Colloïdes, Verres et Nanomatériaux, UMR 5587, Université Montpellier 2 and CNRS, Place Eugène Bataillon,
F-34095 Montpellier Cedex, France*

M. Manna[†]

*Laboratoire de Physique Théorique et Astroparticules, UMR 5207, Université Montpellier 2 and CNRS, Place Eugène Bataillon,
F-34095 Montpellier Cedex, France*

We study the linear stability of an air front pushing on a viscoelastic upper convected Mawxell fluid inside a Hele-Shaw cell. Both theory and experiments involving several viscoelastic fluids prove that a unique dimensionless time parameter $\widetilde{\lambda}$ controls all elastic effects. For small values of $\widetilde{\lambda}$, Newtonian behavior dominates, while for higher values of $\widetilde{\lambda}$ viscoelastic effects appear. We show that the linear growth rate of a small initial perturbation diverges for a critical value $\widetilde{\lambda} = \widetilde{\lambda_c} \simeq \mathbf{10}$. Experiments prove that this divergence is associated to a fracturelike pattern instability of the interface. We conclude that the observed fractures come from the Saffman-Taylor instability and that they directly emerge from the linear regime of it.

PACS number(s): 47.15.gp, 47.15.Fe, 47.20.Ma

I. INTRODUCTION

Saffman-Taylor instability arises when a fluid is pushed on to a more viscous fluid between closely spaced parallel plates [1,2]. The interface between the fluids develops a hydrodynamic instability leading to the formation of fingerlike patterns. That phenomenon is called viscous fingering and it is well known, both theoretically and experimentally when both fluids are Newtonian [3,4]. It has been reported that if the invaded fluid is not Newtonian, there happens an unexpected propagation of fractures through it [5–8].

The shape of the fracturelike patterns has been theoretically investigated [9–11] but very little is known about the origin of those fractures [12,13]. A general physical explanation of fracture nucleation is still lacking. In this paper, by considering the upper convected Maxwell model [14,15], we extend the pioneer work of Wilson [12] and provide an analytical theory for the linear Saffman-Taylor instability of viscoelastic fluids. We have also made experiments on the stability of viscoleastic interfaces when air is injected in a Hele-Shaw cell. Those experiments reproduce quantitatively the main features of our theoretical predictions. The wavelength disturbance of the maximum growth rate gets shifted due to the fluid elasticity. Furthermore, a blow up of the growth rate of the instability is predicted above a critical value of the unique control parameter of the instability, and above this value fractures appear in the experiments. The study is relevant to any theoretical treatment aiming to bridge the gap between the different formalisms proper to viscous liquids and elastic solids.

II. GENERAL FRAMEWORK

It was predicted that an initial flat interface between a Newtonian fluid of viscosity η and air is linearly unstable in a Hele-Shaw cell [3,4,16]. An oscillatory perturbation with time-dependent amplitude $\epsilon \exp(\omega t)$ and arbitrary wave number k is applied to the flat interface. ϵ is small and ω is the amplification rate which depends on k. The front is stable for $\omega < 0$ and unstable for $\omega > 0$. Solid line in Fig. 3(a) shows $\omega(k)$. For a given pressure gradient the perturbation of maximum growth rate has the finite value $\omega_{max} = b^2(-P^0_{,x})^{3/2}/(18 \eta \sqrt{3 \gamma})$ with wave number $k_c = \sqrt{-P^0_{,x}/(3 \gamma)}$ corresponding to the most unstable wavelength $l_c = 2\pi/k_c$ (where γ is the fluid surface tension, $P^0_{,x}$ is the applied pressure gradient, and b is the gap of the cell). Beyond the linear regime, the instability of the front leads to fingerlike patterns.

In the following, we consider viscoelastic fluids instead of Newtonian fluids. A viscoelastic fluid responds essentially as an elastic body if the time scale of a flow event is much shorter than the time scale of the structural reorganizations within the fluid. It responds as a liquid in the opposite case (large time scale). In order to investigate the effect of viscoelasticity on the instability, we consider Maxwellian fluids, i.e., fluids with an unique relaxation time λ. Viscoelastic effects in the Saffman-Taylor instability are expected to be relevant if the maximum growth rate ω_{max} is of the order $1/\lambda$, i.e., when $\lambda \cdot \omega_{max}$ is not much smaller than unity. Straightforwardly, we define a reduced relaxation time for the fluid as

$$\widetilde{\lambda} = 18\sqrt{3}\lambda \omega_{max} = \frac{b^2(-P^0_{,x})^{3/2}}{G\gamma^{1/2}}.$$

The scaling factor $18\sqrt{3}$ is introduced for numerical convenience. Viscoelastic outcomes are then awaited for $\widetilde{\lambda}$ of order of unity or larger [17]. We also introduce a reduced growth rate and a reduced wave vector,

$$\widetilde{k} = \frac{k}{\sqrt{3}k_c} = \sqrt{-\frac{\gamma}{P^0_{,x}}}k,$$

[*]smora@univ-montp2.fr
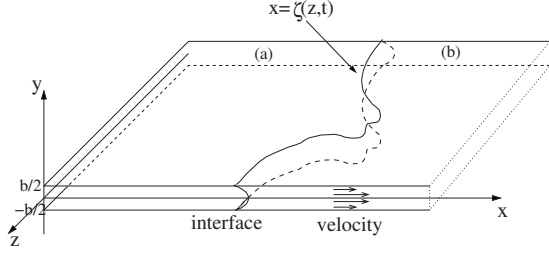
[†]manna@lpta.univ-montp2.fr

FIG. 1. Sketch of the Hele-Shaw cell.

$$\widetilde{\omega} = \frac{\omega}{18\sqrt{3}\,\omega_{max}} = \frac{\eta\gamma^{1/2}}{b^2(-P_{,x}^0)^{3/2}}\omega. \tag{1}$$

III. THEORY

A. Basic equations

First, we introduce basic equations without any approximations. A model for the motion of an incompressible isothermal viscoelastic fluid is given by

$$\rho\frac{D\mathbf{v}}{Dt} = \nabla \cdot \hat{\tau}', \tag{2}$$

$$\nabla \cdot \mathbf{v} = 0, \tag{3}$$

together with a constitutive equation for the stress tensor $\hat{\tau}'$. Here, $\mathbf{v} = (u, v, w)$ is the velocity field, $D/Dt = \partial_t + \mathbf{v}\cdot\nabla$ is the material derivative, and ρ is the constant density. The velocity gradient is $(\nabla\mathbf{v})_{ij} = \partial_j v_i$. We define the extra stress tensor $\hat{\tau}$:

$$\hat{\tau} = P\hat{\mathcal{I}} + \hat{\tau}', \tag{4}$$

where P is the total pressure and $\hat{\mathcal{I}}$ is the identity matrix. Following the upper convected maxwell Model, the constitutive equation is

$$\overset{\triangle}{\hat{\tau}} + \frac{\hat{\tau}}{\lambda} = 2G\mathcal{D}, \tag{5}$$

with $\mathcal{D} = (\nabla\mathbf{v} + \nabla\mathbf{v}^T)/2$ as the rate-of-strain tensor and

$$\overset{\triangle}{\hat{\tau}} = \frac{\partial\hat{\tau}}{\partial t} + \mathbf{v}\cdot\nabla\hat{\tau} - \{\nabla\mathbf{v}\cdot\hat{\tau} + \hat{\tau}\cdot\nabla\mathbf{v}^T\}.$$

As the upper convected derivative of $\hat{\tau}$ [15,18]. G is the elastic modulus of the fluid and λ is the relaxation time. The viscosity is $\eta = G\lambda$. If the stress variations are slower than λ, the derivative is negligible and then, one obtains the well-known constitutive equation for a Newtonian fluid $\hat{\tau} = 2\eta\mathcal{D}$.

The problem is completed by boundaries conditions. We consider the case where air is pushing a viscoelastic fluid. We choose coordinates so that the two plates of the Hele-Shaw cell correspond to $y = -b/2$ and $y = b/2$ (see Fig. 1). The domain Ω of the fluid can be written as

$$\Omega \begin{cases} \zeta < x < \infty \\ -\dfrac{b}{2} < y < \dfrac{b}{2} \\ -\infty \le z \le \infty. \end{cases} \tag{6}$$

with $x = \zeta(z, t)$ as the interface between the two fluids. Since b is far smaller than any lateral length scale in a Hele-Shaw device, we consider that any y dependence of ζ is not relevant. The interface equation can be written as

$$S(x, z, t) = 0 \quad \text{with} \quad S(x, z, t) = x - \zeta(z, t) = 0.$$

The nonevaporation condition yields

$$\frac{DS}{Dt} = 0 \quad \text{or equivalently} \quad -\zeta_{,t} + u - w\zeta_{,z} = 0 \quad \text{for } x = \zeta(z, t), \tag{7}$$

where $X_{,x}$ is for $\frac{\partial X}{\partial x}$, etc.

The no-slip condition for viscous fluid at a solid boundary yields

$$u = v = w = 0 \quad \text{for } y = \pm\frac{b}{2}. \tag{8}$$

The capillarity effects create a discontinuity of the bulk stress tensor between the two sides of a curved interface given by Laplace's Law:

$$(\hat{\tau} - P\mathcal{I}) \cdot \mathbf{N} = \gamma(\kappa_1 + \kappa_2) \cdot \mathbf{N}, \tag{9}$$

where γ is the surface tension, κ_1 and κ_2 are the two main curvatures of the interface, and $\mathbf{N}$ is the vector normal to the interface of the fluid. Neglecting three dimensional effects such as wetting of the cell's plates [19,20] (see below for a justification), Laplace's equation is averaged over the small gap of the cell [3,12,16] and we get (the brackets $\langle\,\rangle$ mean average over the cell gap):

$$\langle(\hat{\tau} - P\mathcal{I}) \cdot \mathbf{N}\rangle = \langle\gamma\kappa_1 \cdot \mathbf{N}\rangle, \tag{10}$$

with

$$\mathbf{N} = \left(\frac{1}{\sqrt{1 + \zeta_{,z}^2}}, 0, \frac{-\zeta_{,z}}{\sqrt{1 + \zeta_{,z}^2}}\right) \tag{11}$$

and

$$\kappa_1 = \frac{\zeta_{,zz}}{(1 + \zeta_{,z}^2)^{3/2}}. \tag{12}$$

B. Pressure scaling

Equations of Sec. III A simplifies if the pressure is chosen in the range where viscoelastic effects appear.

We first consider a one-dimensional (1D) steady flow in the direction of a constant pressure gradient: $\nabla P = (P_{,x}, 0, P_{,z})$. The velocity field $\mathbf{v} = (u, v, w)$ as well as the extra stress tensor $\hat{\tau}$ can be solved explicitly from Eqs. (2)–(5) without any approximation. The extra stress components are given by

$$\tau_{xx} = \frac{2\lambda P_{,x}^2}{\eta} y^2, \quad \tau_{zz} = \frac{2\lambda P_{,z}^2}{\eta} y^2, \quad \tau_{xy} = P_{,x} y,$$

$$\tau_{yz} = P_{,z} y, \quad \tau_{xz} = \frac{2\lambda P_{,x} P_{,z}}{\eta} y^2, \qquad (13)$$

and the velocity by

$$u = \frac{P_{,x}}{2\eta}\left(y^2 - \frac{b^2}{4}\right), \quad v = 0, \quad w = \frac{P_{,z}}{2\eta}\left(y^2 - \frac{b^2}{4}\right). \quad (14)$$

We consider now an inhomogeneous and nonconstant gradient pressure. Let $\mathcal{P}$ be a characteristic pressure, $\mathcal{L}$ be a lateral length scale, and $\epsilon = b/\mathcal{L}$. Then $P_{,x}$ and $P_{,z}$ scale as $\mathcal{P}/\mathcal{L}$ and $P_{,y}$ as $\mathcal{P}/b$. Equations (14) gives

$$u \propto \frac{\mathcal{P}\mathcal{L}}{\eta}\epsilon^2, \quad v = 0, \quad w \propto \frac{\mathcal{P}\mathcal{L}}{\eta}\epsilon^2, \qquad (15)$$

and from Eqs. (13) one obtains

$$\tau_{xy}, \tau_{zy} \propto \epsilon\mathcal{P} \quad \tau_{xz}, \tau_{xx}, \tau_{zz} \propto \epsilon^2\mathcal{P}^2/G. \qquad (16)$$

From the velocity scaling, one obtains a characteristic time scale: $t \propto \mathcal{L}/u \propto \eta/(\mathcal{P}\epsilon^2)$.

Reynolds Number and Deborah Number (defined as the ratio of the relaxation time and the flow characteristic time scale) are

$$\mathcal{R}e = \frac{\mathcal{P}\mathcal{L}^2\rho}{\eta^2} \quad \text{and} \quad De = \frac{\mathcal{P}}{G}\epsilon^2. \qquad (17)$$

In the next of the paper, Reynolds Number is assumed to be small: $\mathcal{R}e \ll 1$. For Deborah number De of order unity or larger, $\mathcal{P} \sim G/\epsilon^2$ or $\mathcal{P} > G/\epsilon^2$, elastic effects are expected to appear. Within this scaling, projections of Eqs. (2), (3), and (5) simplify for $\epsilon \to 0$ (see Appendix A) and one obtains

$$P_{,x} = \tau_{xx,x} + \tau_{yx,y} + \tau_{zx,z},$$

$$P_{,y} = 0,$$

$$P_{,z} = \tau_{xz,x} + \tau_{yz,y} + \tau_{zz,z},$$

$$u_{,x} + w_{,z} = 0, \qquad (18)$$

and

$$\tau_{xx} + \lambda\{\tau_{xx,t} + u\tau_{xx,x} + w\tau_{xx,z} - 2u_{,y}\tau_{yx} - 2u_{,z}\tau_{zx} - 2\tau_{xx}u_{,x}\} = 0,$$

$$\tau_{xy} + \lambda\{\tau_{xy,t} + u\tau_{xy,x} + w\tau_{xy,z} - u_{,x}\tau_{xy} - u_{,z}\tau_{zy}\} = \eta u_{,y},$$

$$\tau_{xz} + \lambda\{\tau_{xz,t} + u\tau_{xz,x} + w\tau_{xz,z} - u_{,x}\tau_{xz} - u_{,y}\tau_{yz} - u_{,z}\tau_{zz} - \tau_{xx}w_{,x}$$
$$- \tau_{xy}w_{,y} - \tau_{xz}w_{,z}\} = 0,$$

$$\tau_{yy} = 0,$$

$$\tau_{yz} + \lambda\{\tau_{yz,t} + u\tau_{yz,x} + w\tau_{yz,z} - \tau_{yx}w_{,x} - \tau_{yz}w_{,z}\} = \eta w_{,y},$$

$$\tau_{zz} + \lambda\{\tau_{zz,t} + u\tau_{zz,x} + w\tau_{zz,z} - 2w_{,x}\tau_{xz} - 2w_{,y}\tau_{yz} - 2w_{,z}\tau_{zz}\} = 0. \qquad (19)$$

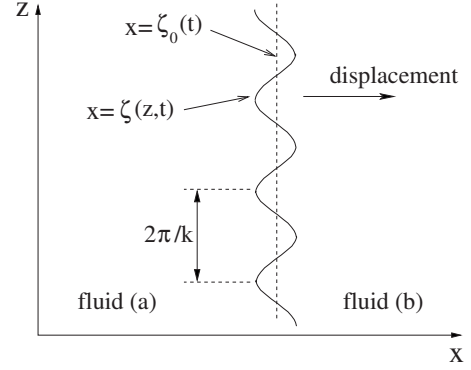FIG. 2. Sinusoidal disturbance of wave vector k.

Finally, stress continuity across the interface yields

$$P - \langle\tau_{xx}\rangle + \zeta_{,z}\langle\tau_{xz}\rangle = \frac{\gamma\zeta_{,zz}}{(1 + \zeta_{,z}^2)^{3/2}}. \qquad (20)$$

C. Disturbance of a straight interface

We consider a linear Hele-Shaw cell. In the basic flow the pressure gradient is along the x-axis $\nabla P = (P_{,x}^0, 0, 0)$. We suppose $P_{,x}^0 < 0$ so that the flow goes from the left ($x < 0$) to the right ($x > 0$). The velocity field and the extra stress tensor are calculated using Eqs. (13) and (14) with $P_{,x} = P_{,x}^0$ and $P_{,z} = 0$. The velocity field is $[u^0(y), 0, 0]$, the extra stress tensor is $\hat{\tau}^0$, and the interface equation is $x = \zeta^0(t)$ with $\zeta^0(t) = \langle u^0\rangle t$. In the perturbated state the velocity field is written as $[u^0(y) + \epsilon u^1(x, y, z; t), 0, \epsilon w^1(x, y, z; t)]$, the pressure as $P^0 + \epsilon P^1(x, z; t)$, the extra stress tensor as $\hat{\tau} = \hat{\tau}^0(y) + \epsilon\hat{\tau}^1(x, y, z; t)$, and the interface equation is $x = \zeta^0(t) + \epsilon\zeta^1(z; t)$. Let us consider a sinusoidal disturbance at $t = 0$ with a wave-vector k (Fig. 2). The aim of the calculation is to find whether the amplitude of the disturbance will grow (unstable situation) or decrease (stable situation). It can be shown that disturbed quantities can be written as

$$\zeta^1(z; t) = \zeta\cos(kz)e^{\omega t},$$

$$u^1(x, y, z; t) = u(y)\cos(kz)e^{\omega t}e^{-\sigma[x - \zeta^0(t)]},$$

$$w^1(x, y, z; t) = w(y)\sin(kz)e^{\omega t}e^{-\sigma[x - \zeta^0(t)]},$$

$$P^1(x, z; t) = P\cos(kz)e^{\omega t}e^{-\sigma[x - \zeta^0(t)]},$$

$$\tau_{xx}^1(x, y, z, t) = \tau_{xx}(y)\cos(kz)e^{\omega t}e^{-\sigma[x - \zeta^0(t)]},$$

$$\tau_{xy}^1(x, y, z, t) = \tau_{xy}(y)\cos(kz)e^{\omega t}e^{-\sigma[x - \zeta^0(t)]},$$

$$\tau_{xz}^1(x, y, z, t) = \tau_{xz}(y)\sin(kz)e^{\omega t}e^{-\sigma[x - \zeta^0(t)]},$$

$$\tau_{yz}^1(x, y, z, t) = \tau_{yz}(y)\sin(kz)e^{\omega t}e^{-\sigma[x - \zeta^0(t)]}.$$

Note that from now ζ, $u(y)$, $w(y)$, P, and $\tau_{ij}(y)$ are the amplitude of the normal modes of the perturbation. We now

rewrite Eqs. (18)–(20) for the (total) perturbed flow. One obtains after linearization with respect to ϵ the following equations:

$$(1 + \lambda\omega - \sigma\lambda u^0)\tau_{xx} - 2\lambda u_{,y}^0 \tau_{xy} = -2\lambda\sigma\tau_{xx}^0 u + 2\lambda\tau_{xy}^0 u_{,y},$$

$$(1 + \lambda\omega - \sigma\lambda u^0)\tau_{xy} = -\lambda\sigma\tau_{xy}^0 u + \eta u_{,y},$$

$$(1 + \lambda\omega - \sigma\lambda u^0)\tau_{xz} - \lambda u_{,y}^0 \tau_{yz} = -\sigma\lambda\tau_{xx}^0 w + \lambda\tau_{xy}^0 w_{,y},$$

$$(1 + \lambda\omega - \sigma\lambda u^0)\tau_{yz} = -\lambda\sigma\tau_{xy}^0 w + \eta w_{,y}, \qquad (21)$$

$$-\sigma P = -\sigma\tau_{xx} + \tau_{xy,y} + k\tau_{xz},$$

$$kP = -\tau_{zy,y} + \sigma\tau_{xz}, \qquad (22)$$

and

$$\zeta P_{,x}^0 + P - \langle\tau_{xx}\rangle = -\gamma k^2 \zeta \quad \text{for } x = \zeta^0 + \zeta^1. \qquad (23)$$

Incompressibility of the fluid yields

$$\sigma u = kw. \qquad (24)$$

D. Stability analysis

From Eqs. (21), (22), and (24), it can be proved that $\sigma = k$ and that the x component of the velocity $u(y)$ is solution of the differential equation (see Appendix B for all the technical aspects)

$$\sigma\left(1 + \lambda\omega - \lambda\sigma\frac{P_{,x}^0}{2\eta}(y^2 - b^2/4)\right)P$$

$$= -\lambda\sigma\left(\frac{2\sigma\lambda P_{,x}^{02}}{\eta}y^2 - P_{,x}^0\right)u + 2\lambda\sigma P_{,x}^0 y u_{,y} - \eta u_{,yy} \qquad (25)$$

with the boundary condition $u(-b/2) = u(b/2) = 0$.

We choose the nondimensionalization introduced is Sec. II: we define

$$\tilde{k} = \sqrt{-\frac{\gamma}{P_{,x}^0}}\,k,$$

$$\tilde{\sigma} = \sqrt{-\frac{\gamma}{P_{,x}^0}}\,\sigma,$$

$$\tilde{\omega} = \frac{\eta\gamma^{1/2}}{b^2(-P_{,x}^0)^{3/2}}\omega, \quad \tilde{\lambda} = \frac{b^2(-P_{,x}^0)^{3/2}}{\eta\gamma^{1/2}}\lambda. \qquad (26)$$

We then obtain

$$\langle u \rangle = \frac{Pb^2\tilde{k}}{\eta}\sqrt{-\frac{P_{,x}^0}{\gamma}}A. \qquad (27)$$

A depends on $\tilde{\lambda}$, $\tilde{\sigma}$, and $\tilde{\omega}$. It can analytically be expanded as a series of powers of $\tilde{\lambda}\tilde{k}$ until an arbitrary order (see again Appendix B for details):
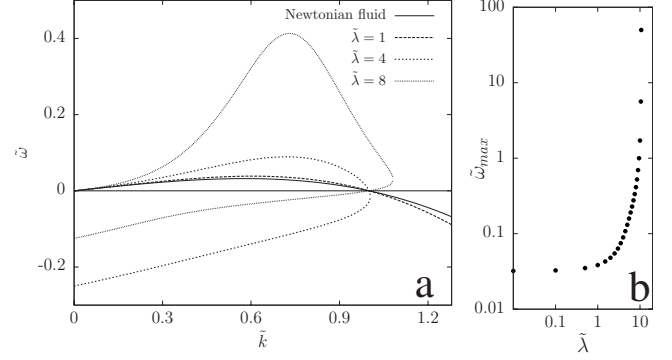

FIG. 3. Theoretical Predictions. (a) Reduced growth rate $\tilde{\omega}$ as a function of reduced wave-vector $\tilde{k}$, for different values of the control parameter $\tilde{\lambda} = b^2(-P_{,x}^0)^{3/2}/G\gamma^{1/2}$. The growth rate for small $\tilde{\lambda}$ is identical to the growth rate for pure Newtonian fluids. (b) maximum value of the growth rate as a function of $\tilde{\lambda}$. Note the divergence for $\tilde{\lambda} \simeq 10.2$.

$$A = \frac{\tilde{\omega}\tilde{\lambda} + 1}{12} - \frac{\tilde{\lambda}\tilde{k}}{120} + \frac{(7\omega\lambda + 8)(\tilde{\lambda}\tilde{k})^2}{20160} + \cdots. \qquad (28)$$

$\langle\tau_{xx}\rangle$ can be calculated in a similar way (see Appendix B):

$$\langle\tau_{xx}\rangle = -2\tilde{k}\tilde{\lambda}PB, \qquad (29)$$

with

$$B = \frac{1}{\tilde{\omega}\tilde{\lambda} + 1}\left[-\frac{\tilde{\omega}\tilde{\lambda} + 2}{12} + \frac{(\omega\lambda + 2)\tilde{\lambda}\tilde{k}}{120}\right.$$

$$\left. -\frac{(11\tilde{\omega}\tilde{\lambda} + 28)(\tilde{\lambda}\tilde{k})^2}{20160} + \cdots\right]. \qquad (30)$$

Note that in the Newtonian limit, $\lambda \rightarrow 0$ and we find $A = 1/12$ and $\tilde{\lambda}B = 0$, as expected for Newtonian fluids.

The continuity of the velocities along (Ox) yields $\langle u \rangle/\omega = \zeta$, and then, from Eq. (23) one obtains

$$\left[\frac{\langle u \rangle P_{,x}^0}{\omega} + P - \langle\tau_{xx}\rangle\right] = -\frac{\gamma k^2 \langle u \rangle}{\omega}, \qquad (31)$$

and [from Eqs. (27), (29), and (31)]

$$\frac{\tilde{k}(1 - \tilde{k}^2)}{\tilde{\omega}}A = 2\tilde{k}\tilde{\lambda}B + 1. \qquad (32)$$

In Fig. 3(a) $\tilde{\omega}$ is plotted [from Eq. (32)]. We have checked that no significant changes appear for powers of $\tilde{\lambda}\tilde{k}$ larger than $\simeq 10.2$ in the series expansions. We observe dramatic elastic effects as soon as $\tilde{\lambda} > 1$. We find a shift in the most unstable wave number and a very sharp increase in the maximum amplification rate. $\tilde{\omega}$ diverges for $\tilde{\lambda} \simeq 10.2$ [see Fig. 3(b)]. Thus, by continuously changing $\tilde{\lambda}$ (for the same fluid and geometry) we obtain curves $\tilde{\omega}(k)$ associated with finger pattern dynamics until the finite value $\tilde{\lambda} \simeq 10.2$ is reached. For that critical value $\tilde{\omega}$ diverges (for a certain value of $\tilde{k}$) and the linear analysis is no longer valid. That corresponds to

TABLE I. Fracture threshold for the investigated fluids. r and Φ are the connectivity and the oil volume fraction. The elastic mudulus G and the relaxation time λ have been measured by classical rheological measurements. $\widetilde{\lambda}_c^{\text{expt.}}$ is the experimental value of the threshold for the fracture.

	Fluid A	Fluid B	Fluid C	Fluid D	Fluid E	Fluid F
ϕ (%); r	2; 4	5; 2.8	14; 2.1	2; 5	3; 4	14; 2.3
G (Pa); λ (s)	4.2; 0.2	13; 0.3	19.5; 0.16	22; 0.6	33; 0.6	39; 0.24
$\widetilde{\lambda}_c^{\text{expt.}}$	10.5 ± 1	10.3 ± 0.7	9.4 ± 0.6	10.0 ± 0.6	9.3 ± 0.4	9.7 ± 0.4

a situation where the perturbation *blows up*.

A shift in the most unstable wave number had been predicted by Wilson [12] who has worked numerically, with another scaling factors and making some unclear assumptions without experimental corroborations. Although Wilson predictions are at first sight similar to the shift we found here the curves do not have the same shape and the blow up of $\widetilde{\omega}$ did not appear. We have found an analytical solution for the growth rate of a viscoelastic fluid leading to a divergence beyond a critical value of $\widetilde{\lambda}$, i.e., beyond a critical value of the pressure gradient for a given fluid, and those results are experimentally corroborated.

IV. EXPERIMENTS

A. Fluids specifications

Most of complex fluids are viscoelastic. But they often have also other non-Newtonian features such as shear thinning, shear thickening, yield stress, etc. In order to investigate viscoelastic outcomes on Saffman-Taylor instability, we choose to work with pure Maxwellian fluids, i.e., fluids with one unique relaxation time associated with an unique elastic modulus. Since it is tempting to perform experiments with $\widetilde{\lambda}$ of order ten, these fluids must be such as it is possible to reach

$$\widetilde{\lambda} = \frac{b^2(-P_{,x}^0)^{3/2}}{G\gamma^{1/2}} \sim 10. \tag{33}$$

For a standard Hele-Shaw cell ($b \sim 500$ μm). For most of the fluids, the surface tension is $\gamma \sim 30$ mN/m. A typical value for the pressure gradient is $P_{,x}^0 \sim 5 \times 10^5$ Pa/m (corresponding to a pressure of air injection $\mathcal{P} \sim 0.5 \times 10^5$ Pa over 10 cm). From Eq. (33) one obtains $G \sim 45$ Pa. The typical value of the Weissenberg number (the product of the inverse of the shear rate and the relaxation time of the fluid) is, within the previous conditions,

$$\text{We} = \lambda u_{,y}^0 \sim \frac{P_{,x}^0 b}{8G} \sim 0.7. $$

Wilson [12] concluded by stating that no direct comparison between experiments and his theory is possible because very little was known about the rheological behavior of the available fluids. In the past two decades, achievements of transient networks provided new viscoelastic fluids [21,22]. However, the elastic modulus of these fluids are often larger than 100 Pa and they behave like pure Maxwellian fluids for

Weissenberg number only smaller than 1 or less. To our knowledge, the only system that is Maxwellian over a wide range of Weissenberg number are bridged microemulsion. Furthermore, the elastic modulus can be chosen to be as small as few Pascal.

Then, we used a fluid composed of an oil-in-water droplet microemulsion (volume fraction ϕ) where the drops are connected to each other by a telechelic polymer [23,24]. The telechelic polymers have a hydrophilic backbone (polyethylene oxide), with a hydrophobic group (18 CH$_2$ groups) at both ends. Those end chains stick reversibly into the hydrophobic core of the oil droplets as it is shown in Fig. 4. We define the connectivity r as the average number of hydrophobic stickers per droplet. The adhesion energy of a sticker in oil droplets is moderate ($\sim 20 k_B T$) so that they randomly escape from time to time and reconnect to any accessible droplet and the topography of the network is permanently renewed, allowing stress relaxation and flow [25,26]. Relaxation time λ is then related to the residence time of a sticker into an oil droplet. Bridged microemulsions have been widely studied in our group in the last decade, including full rheological survey [24,27,28], light [27] and neutron [23] scattering, and numerical simulations [24,29].

The upper convected Maxwell model accurately describes the rheological properties of these fluids. Elastic modulus G and relaxation time λ have been measured by standard linear rheological tests performed with an Ares-RFS controlled-strain rheometer at 23 °C (Table I). Consistently with the upper convected Maxwell model [14], the shear stress τ_{yz} measured in a steady state increases linearly with the shear rate $\dot{\gamma}$ ($\tau_{yz} = G\lambda\dot{\gamma}$) and the first normal stresses difference does it quadratically ($N_1 = 2G\lambda^2\dot{\gamma}^2$) (Fig. 4). Of course, this is true within a certain range of Weissenberg numbers (up to 5). We have checked that Weissenberg Numbers involved in the Hele-Shaw apparatus are inside the Maxwellian range.

Furthermore, rheological properties of these fluids (G and λ) can be precisely tuned by changing droplets concentration or network connectivity.

B. Experimental setup

The fluid is injected into a Hele-Shaw cell (made of two 5-mm-thick square glass plates, 15×15 cm^2; a gap $b = 0.5$ mm between the two plates is fixed by a thin Mylar spacer) from a hole (diameter $2a = 6$ mm) drilled at the center of the lower plate. The flat disk of fluid is then pumped from that hole. Depression is obtained by suddenly expanding the volume of a 80 mL syringe from V_i to V_f. Using
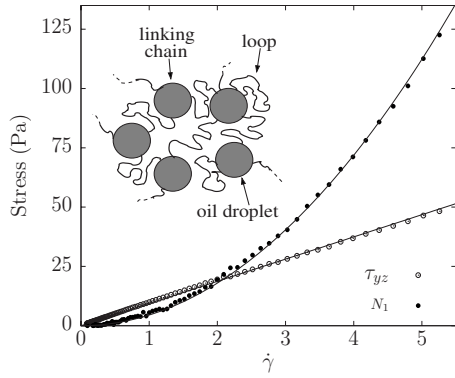
FIG. 4. Rheological properties of fluids. Shear stress (τ_{yz}) and normal stress (N_1) versus shear rate for a bridged microemulsion with connectivity $r=2.3$ and oil volume fraction $\phi=14\%$. λ and G have been measured by oscillatory frequency sweep test ($\lambda=0.24$ s and $G=39$ Pa). The continuous lines are calculated from the upper convected Maxwell Model without any fitting parameter. Insert: schema of a bridged microemulsion.

ideal-gas law the constant depression between the surface and the center of the flat disk $\Delta P = P_0 - P$ (with P_0 as the atmospheric pressure and P as the pressure at the center of the cell) is $\Delta P = P_0(1 - V_i/V_f)$. A bright background is placed below the cell providing an uniform illumination. The liquid-air surface is observed from above with a video camera (Fig. 5). The early stage of pattern formation is recorded and the flat disk average radius R is carefully measured ($R \simeq 10$ cm). The instability wavelength is equal to the number of peaks divided by the disk perimeter ($2\pi R$) and the pressure gradient is $\Delta P/[R \log(R/a)]$. Experiments have been carried out for fluids with various elastic moduli G and relaxation times λ (see Table I). For each fluid, several depressions have been tested. As the flat disk radius is much larger than the wavelength of the pattern, we do not expect any effect due to the radial geometry [30].

C. Discussion

As the surface tension of the fluids is almost constant ($\gamma \simeq 30$ mN/m) we can easily calculate, from the measured wavelength, the value of the reduced wave number $\tilde{k}_{max}$ corresponding to the maximum amplification rate. The plot of the measured $\tilde{k}_{max}$ as a function of $\tilde{\lambda}$ (calculated with $P_{,x}^0$, G, b, and γ) gives a master curve in quantitative agreement with the predicted one (Fig. 6). Wetting effects, known to destroy the two dimensional nature of the flow for capillary numbers $Ca(=\eta u^0/\gamma)$ not far smaller than unity [31–34] seem to be negligible. This can be understood by considering Eq. (20): since τ_{xx} increases faster than Ca, the wetting effects are dominated by elastic effects.

The main result is the fracturelike pattern experimentally observed above a critical value of $\tilde{\lambda}^{\text{expt.}}$ (see Fig. 5). Since $\tilde{\lambda}_c^{\text{expt.}} \simeq 10$ (Fig. 5) for every fluid (see table), one concludes that the observed fracture is a direct consequence of the predicted blow up. This blow up being predicted from a linear theory, one have to conclude that there exists a direct rela-
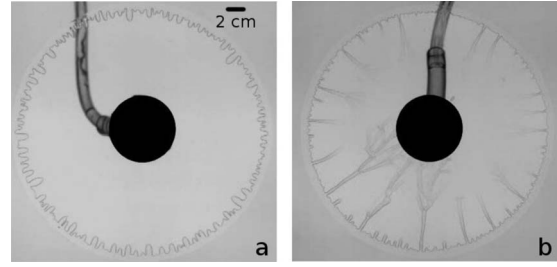

FIG. 5. Pattern formation. (a) Pattern formation for $\tilde{\lambda}=5$. (b) Fracturelike pattern ($\tilde{\lambda}>10.2$).

tionship between the linear regime and the birth of the fractures. This does not prove that fractures nucleate within the nuclear regime. But this proves that the existence of the fractures can be predicted from the physics that takes place within the linear regime. Furthermore, this proves that fracturelike patterns are a consequence of the fluid elasticity (Fig. 6).

V. CONCLUSION

We have theoretically established and quantitatively confirmed by experiments the linear stability of the Saffman-Taylor problem for viscoelastic fluids. The theory successfully describes the transition between viscous to elastic instability.

Fracturelike patterns were associated with a divergence of the maximum growth ratio, which occurs for a finite value of the control parameter. This phenomenon may be related with a kind resonance, as suggested by curves in Fig. 3(a).

Note that since $\tilde{\lambda}$ does not depend on the fluid viscosity, but on the elastic modulus, the blow up is driven by elastic properties. So the present result can be applied even if the viscosity diverges, i.e., for any elastic solids. This study fo-
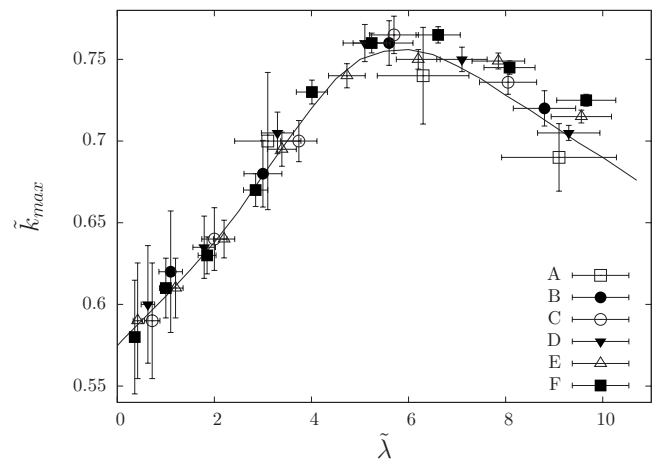

FIG. 6. Reduced wave number as a function of the reduced parameter $\tilde{\lambda}$. Symbols correspond to experimental results and the solid line coresponds to theoretical predictions. Composition and rheological properties of fluids from A to E are given in Table I. Discrepancies observed for large G and $\tilde{k}$ (corresponding to large capillary numbers) may be due to wetting effects.

cused on one aspect of non-Newtonian effects shared by many complex fluids and it could be useful for fluids of practical or industrial interest.

ACKNOWLEDGMENTS

APPENDIX A: SIMPLIFICATION OF THE EQUATION USING THE PRESSURE SCALING

The purpose of this first appendix is to show how to obtain Eqs. (18)–(20) from Eqs. (2), (3), and (5), using the pressure scaling $\mathcal{P} > G/\epsilon^2$ and the Hele-Shaw hypothesis $\epsilon \to 0$.

First we give the expressions of the projections of the basic equations introduced in Sec. III A without any approximation.

Projection of Eqs. (2) and (3) yields

$$u_{,t} + uu_{,x} + vu_{,y} + wu_{,z} = -\frac{1}{\rho}P_{,x} + \frac{1}{\rho}(\tau_{xx,x} + \tau_{yx,y} + \tau_{zx,z}),$$

$$v_{,t} + uv_{,x} + vv_{,y} + wv_{,z} = -\frac{1}{\rho}P_{,y} + \frac{1}{\rho}(\tau_{xy,x} + \tau_{yy,y} + \tau_{zy,z}),$$

$$w_{,t} + uw_{,x} + vw_{,y} + ww_{,z} = -\frac{1}{\rho}P_{,z} + \frac{1}{\rho}(\tau_{xz,x} + \tau_{yz,y} + \tau_{zz,z}),$$

$$u_{,x} + v_{,y} + w_{,z} = 0, \tag{A1}$$

and projection of Eq. (5) yields

$$\tau_{xx} + \lambda\{\tau_{xx,t} + u\tau_{xx,x} + v\tau_{xx,y} + w\tau_{xx,z} - u_{,x}\tau_{xx} - u_{,y}\tau_{yx} - u_{,z}\tau_{zx} \\ - \tau_{xx}u_{,x} - \tau_{xy}u_{,y} - \tau_{xz}u_{,z}\} = 2\eta u_{,x}, \tag{A2}$$

$$\tau_{xy} + \lambda\{\tau_{xy,t} + u\tau_{xy,x} + v\tau_{xy,y} + w\tau_{xy,z} - u_{,x}\tau_{xy} - u_{,y}\tau_{yy} - u_{,z}\tau_{zy} \\ - \tau_{xx}v_{,x} - \tau_{xy}v_{,y} - \tau_{xz}v_{,z}\} = \eta(u_{,y} + v_{,x}), \tag{A3}$$

$$\tau_{xz} + \lambda\{\tau_{xz,t} + u\tau_{xz,x} + v\tau_{xz,y} + w\tau_{xz,z} - u_{,x}\tau_{xz} - u_{,y}\tau_{yz} - u_{,z}\tau_{zz} \\ - \tau_{xx}w_{,x} - \tau_{xy}w_{,y} - \tau_{xz}w_{,z}\} = \eta(u_{,z} + w_{,x}), \tag{A4}$$

$$\tau_{yy} + \lambda\{\tau_{yy,t} + u\tau_{yy,x} + v\tau_{yy,y} + w\tau_{yy,z} - v_{,x}\tau_{xy} - v_{,y}\tau_{yy} - v_{,z}\tau_{zy} \\ - \tau_{yx}v_{,x} - \tau_{yy}v_{,y} - \tau_{yz}v_{,z}\} = 2\eta v_{,y}, \tag{A5}$$

$$\tau_{yz} + \lambda\{\tau_{yz,t} + u\tau_{yz,x} + v\tau_{yz,y} + w\tau_{yz,z} - v_{,x}\tau_{xz} - v_{,y}\tau_{yz} - v_{,z}\tau_{zz} \\ - \tau_{yx}w_{,x} - \tau_{yy}w_{,y} - \tau_{yz}w_{,z}\} = \eta(v_{,z} + w_{,y}), \tag{A6}$$

$$\tau_{zz} + \lambda\{\tau_{zz,t} + u\tau_{zz,x} + v\tau_{zz,y} + w\tau_{zz,z} - w_{,x}\tau_{xz} - w_{,y}\tau_{yz} - w_{,z}\tau_{zz} \\ - \tau_{zx}w_{,x} - \tau_{zy}w_{,y} - \tau_{zz}w_{,z}\} = 2\eta w_{,z}. \tag{A7}$$

Projection of Eq. (9) yields

$$P - \langle\tau_{xx}\rangle + \zeta_{,z}\langle\tau_{xz}\rangle = \frac{\gamma\zeta_{,zz}}{(1 + \zeta_{,z}^2)^{3/2}}, \tag{A8}$$

$$\langle\tau_{yx}\rangle - \langle\tau_{yz}\rangle\zeta_{,z} = 0, \tag{A9}$$

$$\langle\tau_{zx}\rangle + (P - p^*)\zeta_{,z} - \langle\tau_{zz}\rangle\zeta_{,z} = \frac{\gamma\zeta_{,zz}\zeta_{,z}}{(1 + \zeta_{,z}^2)^{3/2}}. \tag{A10}$$

The scaling given by Eqs. (15) and (16) suggest the following nondimensionalization (the nondimensional quantities are overlined):

$$\begin{cases} \tau_{xy} = \epsilon\mathcal{P}\overline{\tau}_{xy} \\ \tau_{zy} = \epsilon\mathcal{P}\overline{\tau}_{zy} \\ \tau_{xz} = \epsilon^2\dfrac{\mathcal{P}^2}{G}\overline{\tau}_{xz} \\ \tau_{xx} = \epsilon^2\dfrac{\mathcal{P}^2}{G}\overline{\tau}_{xx} \\ \tau_{zz} = \epsilon^2\dfrac{\mathcal{P}^2}{G}\overline{\tau}_{zz}. \end{cases} \qquad \begin{cases} u = \dfrac{\mathcal{P}\mathcal{L}}{\eta}\epsilon^2\overline{u} \\ v = 0 \\ w = \dfrac{\mathcal{P}\mathcal{L}}{\eta}\epsilon^2\overline{w} \end{cases} \quad \begin{aligned} t &= \dfrac{\eta}{\mathcal{P}}\dfrac{\overline{t}}{\epsilon^2} \\ P &= \mathcal{P}\overline{P} \end{aligned}.$$

Following this nondimensionalization Eqs. (A2)–(A7) yield

$$\frac{\mathcal{P}}{G}\overline{\tau}_{xx} - \frac{2\mathcal{P}}{G}\overline{u}_{,y}\overline{\tau}_{xy} + \epsilon^2\left(\frac{\mathcal{P}}{G}\right)^2[\overline{\tau}_{xx,t} + \overline{u}\,\overline{\tau}_{xx,x} + \overline{w}\,\overline{\tau}_{xx,z} - 2\overline{u}_{,x}\overline{\tau}_{xx}] \\ - 2\epsilon^2\left(\frac{\mathcal{P}}{G}\right)^2\overline{u}_{,z}\overline{\tau}_{xz} = 2\overline{u}_{,x},$$

$$\overline{\tau}_{xy} + \frac{\mathcal{P}}{G}\epsilon^2[\overline{\tau}_{xy,t} + \overline{u}\,\overline{\tau}_{xy,x} + \overline{w}\,\overline{\tau}_{xy,z} - \overline{u}_{,x}\overline{\tau}_{xy} - \overline{u}_{,z}\overline{\tau}_{zy}] = \overline{u}_{,y},$$

$$\frac{\mathcal{P}}{G}\overline{\tau}_{xz} - \frac{\mathcal{P}}{G}[\overline{w}_{,y}\overline{\tau}_{xy} + \overline{u}_{,y}\overline{\tau}_{yz}] - \epsilon^2\left(\frac{\mathcal{P}}{G}\right)^2[\overline{u}_{,z}\overline{\tau}_{zz} + \overline{w}_{,x}\overline{\tau}_{xx}] \\ + \epsilon^2\left(\frac{\mathcal{P}}{G}\right)^2[\overline{\tau}_{xz,t} + \overline{u}\,\overline{\tau}_{xz,x} + \overline{w}\,\overline{\tau}_{xz,z} - \overline{u}_{,x}\overline{\tau}_{xz} - \overline{w}_{,z}\overline{\tau}_{xz}] \\ = \overline{u}_{,z} + \overline{w}_{,x},$$

$$\overline{\tau}_{zy} + \frac{\mathcal{P}}{G}\epsilon^2[\overline{\tau}_{zy,t} + \overline{u}\,\overline{\tau}_{zy,x} + \overline{w}\,\overline{\tau}_{zy,z} - \overline{w}_{,z}\overline{\tau}_{zy} - \overline{w}_{,x}\overline{\tau}_{xy}] = \overline{w}_{,y},$$

$$\frac{\mathcal{P}}{G}\overline{\tau}_{zz} - \frac{2\mathcal{P}}{G}\overline{w}_{,y}\overline{\tau}_{zy} + \epsilon^2\left(\frac{\mathcal{P}}{G}\right)^2[\overline{\tau}_{zz,t} + \overline{u}\,\overline{\tau}_{zz,x} + \overline{w}\,\overline{\tau}_{zz,z} - 2\overline{w}_{,z}\overline{\tau}_{zz}] \\ - 2\epsilon^2\left(\frac{\mathcal{P}}{G}\right)^2\overline{w}_{,x}\overline{\tau}_{xz} = 2\overline{w}_{,z}. \tag{A11}$$

Equations (A1) yield

$$\mathcal{R}e\;\epsilon^4(\overline{u}_{,t} + \overline{u}\overline{u}_{,x} + \overline{w}\overline{u}_{,z}) = -\overline{P}_{,x} + \epsilon^2\frac{\mathcal{P}}{G}\overline{\tau}_{xx,x} - \overline{\tau}_{xy,y} - \epsilon^2\frac{\mathcal{P}}{G}\overline{\tau}_{zx,z},$$

$$\overline{P}_{,y} = \epsilon^2(\overline{\tau}_{xy,x} + \overline{\tau}_{zy,z}),$$

$$\mathcal{R}e\ \epsilon^4(\bar{w}_{,t} + \overline{uw}_{,x} + \overline{ww}_{,z}) = -\bar{P}_{,z} + \epsilon^2\frac{\mathcal{P}}{G}\bar{\tau}_{zz,z} - \bar{\tau}_{zy,y} - \epsilon^2\frac{\mathcal{P}}{G}\bar{\tau}_{zx,x},$$

(A12)

and Eq. (A8) yields

$$\bar{P} - \overline{P^*} - \epsilon^2\mathcal{P}\left(\frac{\langle\bar{\tau}_{xx}\rangle}{G} - \frac{\langle\bar{\tau}_{xx}^*\rangle}{G^*}\right) + \epsilon^2\mathcal{P}\bar{\zeta}_{,z}\left(\frac{\langle\bar{\tau}_{xz}\rangle}{G} - \frac{\langle\bar{\tau}_{xz}^*\rangle}{G^*}\right)$$

$$= \frac{\gamma}{L\mathcal{P}}\frac{\bar{\zeta}_{,zz}}{(1+\bar{\varsigma}_{,z}^2)^{3/2}}.$$

(A13)

Here, cross gap direction y is scaled as $y = b\bar{y}$, lateral directions x and z are scaled as $x' = \mathcal{L}x$ and $z' = \mathcal{L}z$, and time as $t' = \epsilon^2\mathcal{P}/\eta$. Although overlines in indexed quantities are dropped, the derivatives are with respect to the nondimensional quantities. Note that from Eq. (A5), $v = 0$ yields $D\tau_{yy}/Dt + \tau_{yy} = 0$ and then $\tau_{yy} = 0$. At this point, the only assumption has been that $v = 0$ (bidimensional flow).

Now, we consider Deborah numbers of order unity or larger: $De \sim 1$ or $De \gg 1$, $\mathcal{P} > G/\epsilon^2$. Equations (A11) and (A12) simplify in the limit $\epsilon \to 0$:

$$\frac{\mathcal{P}}{G}\bar{\tau}_{xx} - \frac{2\mathcal{P}}{G}\bar{u}_{,y}\bar{\tau}_{xy} + \epsilon^2\left(\frac{\mathcal{P}}{G}\right)^2[\bar{\tau}_{xx,t} + \overline{u}\bar{\tau}_{xx,x} + \overline{w}\bar{\tau}_{xx,z} - 2\bar{u}_{,x}\bar{\tau}_{xx}]$$

$$- 2\epsilon^2\left(\frac{\mathcal{P}}{G}\right)^2\bar{u}_{,z}\bar{\tau}_{xz} = 0,$$

$$\bar{\tau}_{xy} + \frac{\mathcal{P}}{G}\epsilon^2[\bar{\tau}_{xy,t} + \overline{u}\bar{\tau}_{xy,x} + \overline{w}\bar{\tau}_{xy,z} - \bar{u}_{,x}\bar{\tau}_{xy} - \bar{u}_{,z}\bar{\tau}_{zy}] = \bar{u}_{,y},$$

$$\frac{\mathcal{P}}{G}\bar{\tau}_{xz} - \frac{\mathcal{P}}{G}[\bar{w}_{,y}\bar{\tau}_{xy} + \bar{u}_{,y}\bar{\tau}_{yz}] - \epsilon^2\left(\frac{\mathcal{P}}{G}\right)^2[\bar{u}_{,z}\bar{\tau}_{zz} + \bar{w}_{,x}\bar{\tau}_{xx}]$$

$$+ \epsilon^2\left(\frac{\mathcal{P}}{G}\right)^2[\bar{\tau}_{xz,t} + \overline{u}\bar{\tau}_{xz,x} + \overline{w}\bar{\tau}_{xz,z} - \bar{u}_{,x}\bar{\tau}_{xz} - \bar{w}_{,z}\bar{\tau}_{xz}] = 0,$$

$$\bar{\tau}_{zy} + \frac{\mathcal{P}}{G}\epsilon^2[\bar{\tau}_{zy,t} + \overline{u}\bar{\tau}_{zy,x} + \overline{w}\bar{\tau}_{zy,z} - \bar{w}_{,z}\bar{\tau}_{zy} - \bar{w}_{,x}\bar{\tau}_{xy}] = \bar{w}_{,y},$$

$$\frac{\mathcal{P}}{G}\bar{\tau}_{zz} - \frac{2\mathcal{P}}{G}\bar{w}_{,y}\bar{\tau}_{zy} + \epsilon^2\left(\frac{\mathcal{P}}{G}\right)^2[\bar{\tau}_{zz,t} + \overline{u}\bar{\tau}_{zz,x} + \overline{w}\bar{\tau}_{zz,z} - 2\bar{w}_{,z}\bar{\tau}_{zz}]$$

$$- 2\epsilon^2\left(\frac{\mathcal{P}}{G}\right)^2\bar{w}_{,x}\bar{\tau}_{xz} = 0,$$

(A14)

$$\bar{P}_{,x} = \epsilon^2\frac{\mathcal{P}}{G}\bar{\tau}_{xx,x} + \bar{\tau}_{xy,y} + \epsilon^2\frac{\mathcal{P}}{G}\bar{\tau}_{zx,z},$$

$$\bar{P}_{,y} = 0,$$

$$\bar{P}_{,z} = \epsilon^2\frac{\mathcal{P}}{G}\bar{\tau}_{zz,z} + \bar{\tau}_{zy,y} + \epsilon^2\frac{\mathcal{P}}{G}\bar{\tau}_{zx,x}.$$

(A15)

Note that Eq. (A13) does not simplify here. Coming back to dimensionalized quantities, one obtains Eqs. (18)–(20) of Sec. III B.

APPENDIX B: DETAILED CALCULCATION OF THE EQUATION OF THE MOTION FOR THE DISTURBANCE

In this appendix we show in detail how the mean velocity [Eq. (27)] and the mean value of τ_{xx} [Eq. (29)] for the disturbance can be calculated from Eqs. (21)–(23).

From Eqs. (21) one obtains

$$(1 + \lambda\omega - \lambda\sigma u^0)\tau_{xy,y} = \lambda\sigma u_{,y}^0\tau_{xy} - \lambda\sigma\tau_{xy}^0 u_{,y} - \lambda\sigma\tau_{xy,y}^0 u$$
$$+ \eta u_{,yy},$$

$$-(1 + \lambda\omega - \lambda\sigma u^0)\sigma\tau_{xx} = -2\sigma\lambda u_{,y}^0\tau_{xy} + 2\lambda\sigma^2\tau_{xx}^0 u$$
$$- 2\lambda\sigma\tau_{xy}^0 u_{,y},$$

$$(1 + \lambda\omega - \lambda\sigma u^0)k\tau_{xz} = \lambda k u_{,y}^0\tau_{yz} - \sigma^2\lambda\tau_{xx}^0 u + \lambda\sigma\tau_{xy}^0 u_{,y}.$$

Adding these three equations, one obtains with Eqs. (22)

$$-\sigma(1 + \lambda\omega - \lambda\sigma u^0)P = -\lambda\sigma u_{,y}^0\tau_{xy} + \lambda k u_{,y}^0\tau_{yz} + \lambda\sigma(\sigma\tau_{xx}^0$$
$$- \tau_{xy,y}^0)u - 2\lambda\sigma\tau_{xy}^0 u_{,y} + \eta u_{,yy}.$$

This equation simplifies since [from Eq. (21)]

$$\tau_{xy} = \frac{\eta u_{,y} - \lambda\sigma\tau_{xy}^0 u}{1 + \lambda\omega - \lambda\sigma u^0} \quad \text{et} \quad \tau_{yz} = \frac{\eta u_{,y} - \lambda\sigma\tau_{xy}^0 u}{1 + \lambda\omega - \lambda\sigma u^0}\left(\frac{\sigma}{k}\right),$$

and one obtains

$$\sigma(1 + \lambda\omega - \lambda\sigma u^0)P = -\lambda\sigma(\sigma\tau_{xx}^0 - \tau_{xy,y}^0)u + 2\lambda\sigma\tau_{xy}^0 u_{,y}$$
$$- \eta u_{,yy}.$$

(B1)

On an other hand, considering again Eqs. (21) one obtains

$$-(1 + \lambda\omega - \lambda\sigma u^0)\tau_{yz,y} = -\sigma\lambda u_{,y}^0\tau_{yz} + \lambda\sigma\tau_{xy,y}^0 w + \lambda\sigma\tau_{xy}^0 w_{,y}$$
$$- \eta w_{,yy},$$

$$\sigma(1 + \lambda\omega - \lambda\sigma u^0)\tau_{xz} = \sigma\lambda u_{,y}^0\tau_{yz} - \sigma^2\lambda\tau_{xx}^0 w + \lambda\sigma\tau_{xy}^0 w_{,y}.$$

Adding these equations, one obtains with Eqs. (22)

$$\frac{k^2}{\sigma}(1 + \lambda\omega - \lambda\sigma u^0)P = -\lambda\sigma(\sigma\tau_{xx}^0 - \tau_{xy,y}^0)u + 2\lambda\sigma\tau_{xy}^0 u_{,y}$$
$$- \eta u_{,yy}.$$

(B2)

From Eqs. (B1) and (B2),

$$\sigma = \pm k.$$

Since the perturbation must not diverge for $x \to +\infty$: $\sigma = +k$.

Substituting in Eq. (B1) the expression of $u^0(y)$, $\tau_{xx}^0(y)$, and τ_{xy}^0 one obtains a differential equation for $u(y)$:

$$k\left(1 + \lambda\omega - \lambda k\frac{P_{,x}^0}{2\eta}(y^2 - b^2/4)\right)P$$

$$= -\lambda k\left(\frac{2k\lambda P_{,x}^{02}}{\eta}y^2 - P_{,x}^0\right)u + 2\lambda k P_{,x}^0 y u_{,y} - \eta u_{,yy}.$$

(B3)

We choose nondimensionalization given by Eqs. (26), and we define $Y = y/b$. Equation (B3) becomes

$$\sqrt{-\frac{P_{,x}^0}{\gamma}}\frac{Pb^2\widetilde{k}}{\eta}\left[1+\widetilde{\lambda}\widetilde{\omega}+\frac{1}{2}\widetilde{\lambda}\widetilde{k}\left(Y^2-\frac{1}{4}\right)\right]$$

$$=-\widetilde{\lambda}\widetilde{k}[2\widetilde{\lambda}\widetilde{k}Y^2+1]u-2\widetilde{\lambda}\widetilde{k}Yu_{,Y}-u_{,YY}. \qquad \text{(B4)}$$

The boundaries condition are $u(Y=-1/2)=u(Y=1/2)=0$. To solve this differential equation, we write the solution as

$$u(Y)=\frac{Pb^2\widetilde{k}}{\eta}\sqrt{-\frac{P_{,x}^0}{\gamma}}(a_0(Y)+a_1(Y)\widetilde{\lambda}\widetilde{k}+a_2(Y)(\widetilde{\lambda}\widetilde{k})^2$$

$$+a_3(Y)(\widetilde{\lambda}\widetilde{k})^3+a_4(Y)(\widetilde{\lambda}\widetilde{k})^4+\cdots).$$

Function $a_0(Y)$, $a_1(Y)$, $a_2(Y)$, etc. can easily be computed using the differential equations

$$-(1+\widetilde{\omega}\widetilde{\lambda})=a_0'',$$

$$-\frac{1}{2}\left(y^2-\frac{1}{4}\right)=a_0+2ya_0'+a_1'',$$

$$2y^2a_0+a_1+2ya_1'+a_2''=0,$$

$$2y^2a_1+a_2+2ya_2'+a_3''=0,$$

$$2y^2a_2+a_3+2ya_3'+a_4''=0,$$

$$2y^2a_3+a_4+2ya_4'+a_5''=0,$$

$$2y^2a_4+a_5+2ya_5'+a_6''=0,$$

$$2y^2a_5+a_6+2ya_6'+a_7''=0,$$

$$\cdots$$

This system can be solved at any order in $\widetilde{\lambda}\widetilde{k}$. $\langle u\rangle$ is obtained by integrating $u(Y)$ from $Y=-1/2$ to $Y=1/2$.

We calculate now $\tau_{xx}(y)$. Following the first equation of Eqs. (21), one obtains

$$\tau_{xx}=-\frac{2\widetilde{\lambda}\eta\gamma^{1/2}}{b^2(-P_{,x}^0)^{1/2}}\frac{y}{1+\widetilde{\omega}\widetilde{\lambda}+\frac{\widetilde{\lambda}\widetilde{k}}{2}(y^2-1/4)}$$

$$\times\left\{\frac{u_{,Y}+\widetilde{\lambda}\widetilde{k}yu}{1+\widetilde{\omega}\widetilde{\lambda}+\frac{\widetilde{\lambda}\widetilde{k}}{2}(y^2-1/4)}+2\widetilde{\lambda}\widetilde{k}yu+u_{,Y}\right\}$$

$$=-2\widetilde{k}P\frac{y}{1+\widetilde{\omega}\widetilde{\lambda}+\frac{\widetilde{\lambda}\widetilde{k}}{2}(y^2-1/4)}$$

$$\times\left\{\frac{a_{,y}+\widetilde{\lambda}\widetilde{k}ya}{1+\widetilde{\omega}\widetilde{\lambda}+\frac{\widetilde{\lambda}\widetilde{k}}{2}(y^2-1/4)}+2\widetilde{\lambda}\widetilde{k}ya+a_{,y}\right\}.$$

Knowing $u(y)$, τ_{xx} can be expanded as

$$\tau_{xx}=-2\widetilde{k}\widetilde{\lambda}P\overbrace{(b_0(y)+b_1(y)\widetilde{\lambda}\widetilde{k}+b_2(y)(\widetilde{\lambda}\widetilde{k})^2+b_3(y)(\widetilde{\lambda}\widetilde{k})^3+b^4(y)(\widetilde{\lambda}\widetilde{k})^4+\cdots)}^{=b(y)},$$

$b_0(y)$, $b_1(y)$, $b_2(y)$, etc., can be easily calculated with the $a_i(y)$ functions.

[1] S. Hill, Chem. Eng. Sci. **1**, 247 (1952).

[2] P. Saffman and G. I. Taylor, Proc. R. Soc. London, Ser. A **245**, 312 (1958).

[3] R. Chuoke, P. Van Meurs, and C. Van der Pol, Petrol. Trans. AIME **216**, 188 (1959).

[4] D. Bensimon, L. Kadanoff, S. Liang, B. Shraiman, and C. Tang, Rev. Mod. Phys. **58**, 977 (1986).

[5] J. Nittmann, G. Daccord, and H. Stanley, Nature (London) **314**, 141 (1985).

[6] H. Van Damme, H. Obrecht, P. Levitz, L. Gatineau, and C. Laroche, Nature (London) **320**, 731 (1986).

[7] H. Zhao and J. V. Maher, Phys. Rev. E **47**, 4278 (1993).

[8] J. Nase, A. Lindner, and C. Creton, Phys. Rev. Lett. **101**, 074503 (2008).

[9] A. Levermann and I. Procaccia, Phys. Rev. Lett. **89**, 234501 (2002).

[10] M. Ben Amar and C. Corvera-Poiré, Phys. Fluids **11**, 1757 (1999).

[11] M. Ben Amar, Phys. Rev. E **51**, R3819 (1995).

[12] S. Wilson, J. Fluid Mech. **220**, 413 (1990).

[13] P. de Gennes, Europhys. Lett. **3**, 195 (1987).

[14] C. Macosko, *Rheology: Principles, Measurements, and Applications* (Wiley-VCH, New York, 1994).

[15] G. Astarita and G. Marrucci, *Principles of Non-Newtonian Fluid Mechanics* (McGraw-Hill, New York, 1974).

[16] G. Batchelor, H. Moffatt, and M. Worster, *Perspectives in Fluid Dynamics* (Cambridge University Press, New York, 2000).

[17] S. Mora and M. Manna, Phys. Rev. E **80**, 016308 (2009).

[18] D. Joseph, *Fluid Dynamics of Viscoelastic Liquids* (Springer-Verlag, New York, 1990).

[19] C. Park and G. Homsy, J. Fluid Mech. **139**, 291 (1984).

[20] L. Paterson, Phys. Fluids **28**, 26 (1985).

[21] T. Annable, R. Buscall, R. Ettelaie, and D. Whittlestone, J. Rheol. **37**, 695 (1993).

[22] J. Berret, D. Roux, and G. Porte, J. Phys. II **4**, 1261 (1994).

[23] M. Filali, R. Aznar, M. Svensson, G. Porte, and J. Appell, J. Phys. Chem. **103**, 7293 (1999).

[24] F. Molino, J. Appell, M. Michel, G. Porte, S. Mora, and E. Sunyer, J. Phys.: Condens. Matter **12**, A491 (2000).

[25] F. Tanaka and S. Edwards, Non-Newtonian Fluid Mech. **43**, 273 (1992).

[26] M. Green and A. Tobolsky, J. Chem. Phys. **14**, 80 (1946).

[27] E. Michel, M. Filali, R. Aznar, G. Porte, and J. Appell, Langmuir **16**, 8702 (2000).

[28] M. Filali, E. Michel, S. Mora, F. Molino, and G. Porte, Colloids Surf., A **183**, 203 (2001).

[29] P. I. Hurtado, L. Berthier, and W. Kob, Phys. Rev. Lett. **98**, 135503 (2007).

[30] L. Paterson, J. Fluid Mech. **113**, 513 (1981).

[31] P. Tabeling and A. Libchaber, Phys. Rev. A **33**, 794 (1986).

[32] P. Saffman, J. Fluid Mech. **173**, 73 (1986).

[33] T. Maxworthy, Phys. Rev. A **39**, 5863 (1989).

[34] M. W. DiFrancesco and J. V. Maher, Phys. Rev. A **40**, 295 (1989).